J Mater Sci (2007) 42:6590–6599
DOI 10.1007/s10853-007-1500-6

Blending properties of poly(vinyl alcohol) and nylon 6-clay nanocomposite blends

Jen-Taut Yeh · Peng Xu · Fang-Chang Tsai

Received: 19 October 2006 / Accepted: 5 January 2007 / Published online: 27 April 2007

Abstract An investigation of the blending, rheological and tensile properties of poly(vinyl alcohol) (PVA) and nylon 6 clay (NYC) nanocomposite blends was conducted. The characteristics of melting endotherm, X-ray diffraction patterns of α form PVA crystals and hydrogen-bonded hydroxyl groups originally associated with the PVA resin almost disappear after blending less than 16.7 wt% of PVA in NYC resins. However, the characteristics of melting endotherm, X-ray diffraction of α form PVA crystals and hydrogen-bonded hydroxyl groups originally associated with the PVA resins appear gradually as the PVA contents of NYC/PVA specimens are more than 16.7 wt%. The torques vs. time measurements and tensile properties of NYC/PVA specimens support the ideas that PVA molecules are miscible with PA molecules to some extents in the molecular level as the PVA contents of NYC/PVA specimens are less than 16.7 wt%. Moreover, the additional demarcated humps and significantly increased torques and ''stabilized'' time values support the presence of separated PVA phases in NYC/PVA specimens as their PVA contents are more than 50 wt%. On the other hand, the α form PA crystals continue to grow at the expense of γ form PA crystals as the PVA contents of NYC/PVA specimens increase, and the characteristics of the γ form PA crystals originally shown on the melting endotherm and X-ray diffraction patterns of the NYC resin can barely be seen as the PVA contents of NYC/PVA specimens are equal to or more than 50 wt%. Possible reasons accounting for these interesting blending properties are proposed.

J.-T. Yeh · P. Xu
Faculty of Chemistry and Material Science, Hubei University, Wuhan, China

J.-T. Yeh (✉) · F.-C. Tsai
Graduate School of Polymer Engineering, National Taiwan University of Science and Technology, Taipei, Taiwan
e-mail: jyeh@tx.ntust.edu.tw

J.-T. Yeh
Department of Textile Engineering, Nanya Institute of Technology, Jungli, Taiwan

Introduction

There has been considerable interest in polymer blends in recent decades, owing to their better combination of physical properties and potential applications than those of the homo-polymers [1–3]. It is generally recognized that the properties of polymer blends are greatly dependent on their miscibility and phase behavior. Therefore, the miscibility and phase behavior of polymer blends has been the subject of numerous studies [2, 4].

Poly(vinyl alcohol) (PVA) is well known for its low cost, excellent transparency, flexibility, toughness, biodegradability, and gas barrier properties, and hence, widely used as, textile sizing and/or finishing agent, emulsifier, photosensitive coating, food packaging and/or adhesives for paper, wood, textiles and leather [5–8]. However, PVA can seldom be used as a thermoplastic polymer, because of its high water absorption and weak thermal stability. In contrast, PVA can be used as the modifier added in other polymers through melt-blending process [9–11], since blend preparation is the best and economically viable option to modify the plastics. Ikejima and coauthors [9] found that the biodegradation rates of poly(3-hydroxybutyric acid) (PHB) can be significantly accelerated after blending of small amounts of PVA resins, in which PVA/PHB

blends can be processed as the optically clear films. On the other hand, Gajria et al. [10] exposed that the tensile properties of Poly(lactic acid) (PLA) can be improved significantly after melt-blending 5–30 wt% of PVA resins. They suggested that PLA is compatible with PVA at these compositions, since only one glass transition temperature was observed in the DSC thermograms of the PLA/PVA blends. On the other hand, after melt-blending 25 wt% of PVA in nylon 6 resins, Koulouri and Kallitsis [11] found that the elongation at break (ε_b) of nylon 6/PVA blends reaches 640%, which is significantly higher than that of the pure nylon 6 specimen (i.e., 580%). They further exposed that nylon 6 are compatible with PVA at this composition, since only one glass transition temperature was found by the DMTA analysis of the nylon 6/PVA blend. In contrast, at other PVA contents, the ε_b values of the nylon 6/PVA blends were significantly lower than that of the pure nylon 6 specimens and more than one glass transition temperature were found by their DMTA analysis.

Modification of the barrier and physical properties of polymers using nanoscale filler particles with a high surface area to thickness aspect ratio has drawn much attention recently [12, 13], wherein the filler particles (e.g., smectite clays) are typically approximately 1 nm thick with laterally dimensions of the order 200–1000 nm. Significant improvements in modulus and heat deflection temperature were first found in nylon 6 clay nanocomposite (NYC) by addition of 2–8 wt% of smectite clays [13, 14]. Later investigations found that the polymer nanocomposites exhibit significant better barrier performance to diffusing species in comparison with the unmodified polymers [12, 13, 15, 16]. Presumably, this improvement in barrier properties of polymers is based on the tortuosity arguments, wherein the permeant molecules must travel the longer diffusive path in presence of the clay fillers [17–22]. However, as far as we know, no investigation has ever been reported on the melt-blending and physical properties of NYC/PVA blends. In order to serve PVA as a better thermoplastic resin while still maintain some of their excellent properties (e.g., mechanical and barrier properties), PVA were melt-blended with NYC instead of PA in this study, wherein the presence of clay fillers in PA is expected to further enhance the barrier properties of the PVA/NYC blends. However, film-blowing or extrusion of the clay fillers contained NYC and NYC melt-blended resins are often difficult and ended up with ruptured and poor transparency of the films. As suggested by several investigators [23–25], protonated amino end groups of the PA molecules can be ionically bonded to the surfaces of negatively charged silicate sheets, which then leads to a poorly arranged PA conformation gathered on the surfaces of the silicate sheets. These poorly arranged PA molecules are then served as the nucleation sites, and hence, cause the formation of γ form PA crystals during the crystallization processes of NYC melts, although the form PA crystals with PA molecules linearly aligned in the unit cells are the more stable form. Presumably, the poor process ability of the NYC and NYC blends can be correlated with the poorly arranged PA conformation and its resulted melt structure.

The main objective of this study is to investigate the blending, rheological and tensile properties of NYC/PVA blends. The blending properties of NYC/PVA blends prepared with varying compositions were investigated. It is worth noting that the α form PA crystals continue to grow at the expense of γ form PA crystals as the PVA contents of NYC/PVA specimens increase, and the characteristics of the γ form PA crystals originally shown on the melting endotherm and X-ray diffraction patterns of the NYC resin can barely be seen as the PVA contents of NYC/PVA specimens are equal to or more than 50 wt%. In order to understand the compatibility of NYC and PVA resins in the molecular level, the rheological, thermal, X-ray diffraction, Fourier-transform infrared and tensile properties of NYC/PVA blends were carried out. Possible reasons accounting for the interesting blending properties of the NYC/PVA blends are proposed.

Experimental

Materials and sample preparation

Poly(vinyl alcohol) (PVA) and Nylon 6 clay (NYC) resins used in this study were obtained from Nippon Gohsei Corporation (Tokyo, Japan) and Unitika LTD., (Tokyo, Japan), respectively, wherein PVA and NYC had a trade name and quoted average molecular weight (Mw) of AX-2000/74,800 and M1030D/62,000, respectively. The NYC nanocomposite contains 4.6 wt% exfoliated layered silicate and is made by in-situ hydrolytic polymerization of ε-caprolactam in the presence of swollen organically modified silicate. The NYC/PVA specimens were prepared by melt blending the NYC and PVA resins using a SU-70 Plasti-Corder Mixer, which was purchased from Suyuan science and Technology Corporation, Chang Zhou, China. The 70 mL Plasti-Corder Mixer is equipped with a co-rotating, intermeshing twin screw with a diameter of 30 mm and L/D ratio of 10. Before melt-blending, the NYC and PVA resins were dried in a vacuum oven at 80 °C for 16 and 12 h, respectively. The dried components of NYC/PVA at varying weight ratios were then melt-blended at 240 °C /250 rpm for 4 min in the Plasti-Corder Mixer. The fully blended NYC/PVA components were then cooled at room temperature. The compositions of the NYC/PVA specimens prepared in this study are summarized in Table 1.

Table 1 The compositions of NYC/PVA specimens

Sample	NYC (%)	PVA (%)
NYC	100	0
NYC_7PVA_1	87.5	12.5
NYC_5PVA_1	83.3	16.7
NYC_3PVA_1	75.0	25.0
NYC_2PVA_1	66.7	33.3
NYC_1PVA_1	50.0	50.0
NYC_1PVA_2	33.3	66.7
NYC_1PVA_3	25.0	75.0
PVA	0	100

Rheological properties

The torques vs. time measurements of the NYC/PVA specimens were carried out in the Plasti-Corder Mixer equipped with a torque measurement device. The rotational speed was set at 250 rpm and the temperature was controlled at 240 °C.

Wide angle X-ray diffraction

The wide angle X-ray diffraction (WAXD) properties of NYC, PVA and NYC/PVA specimens were determined using a Siemens D5000D diffractometer equipped with a Ni-filtered CuKα radiation operated at 35 kV and 25 mA. Each specimen with 1 mm thickness was maintained stationary at 25 °C and scanned in the reflection mode from 2 to 40° at a scanning rate of 5° min^{-1}.

Thermal properties

The thermal properties of NYC, PVA and NYC/PVA resins were determined at 25 °C using a Du Pont 2010 differential scanning calorimetry (DSC) (Table 2). All scans were carried out at a heating rate of 20 °C/min and under flowing nitrogen of a flow rate of 25 mL/min. The instrument was calibrated using pure indium. Samples weighing about 0.5 mg were placed in standard aluminum sample pans for each DSC experiment.

Table 2 Thermal properties of NYC, PVA and NYC/PVA resins

Sample	Peak temperature (°C) associated with NYC and PVA melting endotherms		
	NYC	PVA	
NYC	214.0		
NYC_7PVA_1	213.2	219.7	–
NYC_5PVA_1	213.3	220.1	–
NYC_3PVA_1	214.8	220.8	228.2
NYC_2PVA_1	214.9	221.0	228.4
NYC_1PVA_1	–	221.7	228.5
NYC_1PVA_2	–	221.8	228.9
NYC_1PVA_3	–	–	227.9
PVA			230.9

Fourier transform infrared spectroscopy (FT–IR)

Fourier transform infrared spectroscopic measurements of NYC, PVA and NYC/PVA specimens were recorded on a Nicolet Avatar 320 FT–IR spectrophotometer at 25 °C, wherein 32 scans with a spectral resolution 1 cm^{-1} were collected during each spectroscopic measurement. Infrared spectra of the film specimens were determined by using the conventional NaCl disk method. The 1,1,1,3,3,3-hexafluoro-2-propanol solutions containing the NYC, PVA and NYC/PVA were cast onto NaCl disk and dried at 60 °C for 30 min, respectively. The cast films used in this study were prepared sufficiently thin enough to obey the Beer-Lambert law.

Mechanical properties

The tensile properties of the hot-pressed NYC, PVA and NYC/PVA specimens were determined using a Shimadzu tensile testing machine model AG-10KNA at 25 °C and a crosshead speed of 200 mm/min. A 35 mm gauge length was used during each tensile experiment. The dimensions of the dog-bone shaped specimens were prepared according to ASTM D638 type IV standard. The values of tensile strength and elongation at break were obtained based on the average tensile results of at least five tensile specimens.

Results and discussion

Rheological properties

Figure 1 summarized plots of the torque vs. mixing time of NYC, PVA and NYC/PVA specimens at 240 °C. Similar to most of the polymers, the torques values of the NYC, PVA and NYC/PVA specimens varied initially and then stabilized after a certain period of time during their melting processes. The ''stabilized'' time and torque value of NYC specimen are significantly smaller than those of the PVA specimen. The ''stabilized'' time and torque values of NYC/PVA specimens increase slightly as the PVA contents increase from 0 to 16.7 wt%, however, they increase significantly from 0.75 min/12.3 Nm to 1.25 min/23.1 Nm as the PVA contents increase from 16.7 to 50 wt%, respectively. In fact, at PVA contents more than 50 wt%, another demarcated hump can be observed on plots of the torque vs. mixing time of NYC/PVA specimens

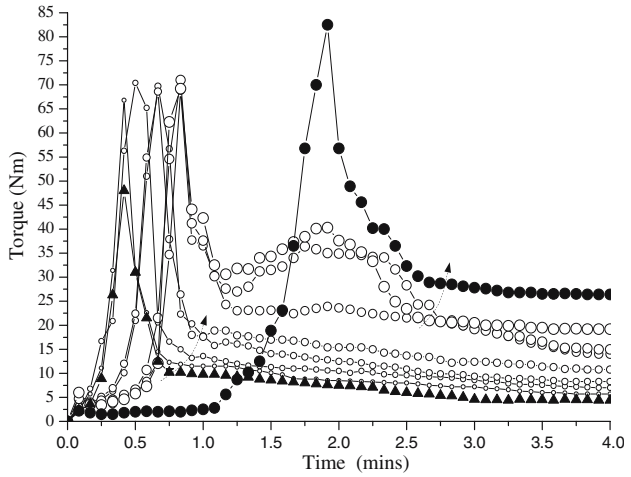

Fig. 1 Plots of torque vs. time of NYC (▲), PVA(●), NYC_7PVA_1 (○), NYC_5PVA_1 (○), NYC_3PVA_1 (○), NYC_2PVA_1 (○), NYC_1PVA_1 (○), NYC_1PVA_2 (○), and NYC_1PVA_3 (○) specimens

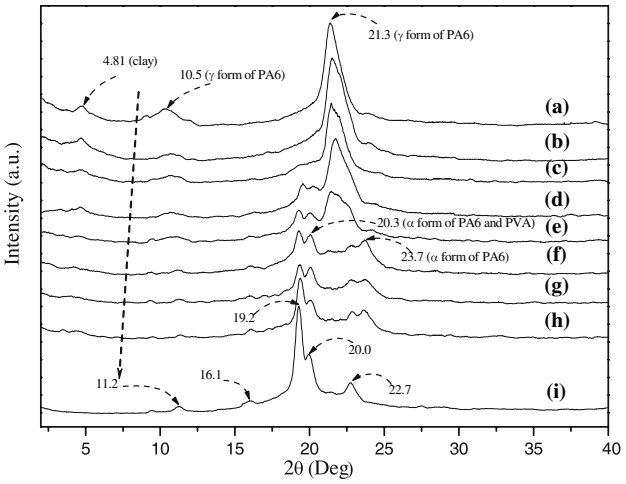

Fig. 2 WAXS diffraction patterns of (**a**) NYC, (**b**) NYC_7PVA_1, (**c**) NYC_5PVA_1, (**d**) NYC_3PVA_1, (**e**) NYC_2PVA_1, (**f**) NYC_1PVA_1, (**g**) NYC_1PVA_2, (**h**) NYC_1PVA_3 and (**i**) PVA specimens

before the mixing time reaches the ''stabilized'' melt-blending status. As shown in Fig. 1, the ''stabilized'' time and torque values of NYC/PVA specimens increase significantly from 1.25 min/23.1 Nm to 2.6 min/23.9 Nm as the PVA contents increase from 50 to 75 wt%. Presumably, these demarcated humps indicate the difficulty of melt-blending of the NYC/PVA specimens with high PVA contents, and hence, require longer time before reaching the stabilized melt-blending status.

Wide angle X-ray diffraction

Typical X-ray diffraction patterns and peak diffraction angles of NYC, PVA and NYC/PVA specimens are shown in Fig. 2. The crystals of PVA specimen crystallized at 25°C are α form crystals, which correspond to a peak X-ray diffraction angle at 11.2°, 16.1°, 19.2°, 20.0° and 22.7° [26]. Similar to the results found in our previous investigations [22], the crystals of NYC specimen crystallized at 25 °C are γ form crystals, which correspond to a peak X-ray diffraction angle at 21.3° [27]. After blending PVA in NYC resins, the characteristics of X-ray diffraction patterns of NYC/PVA specimens are very similar to those of the NYC and PVA specimens, wherein γ form PA crystals and α form PVA crystals are the main crystals present in NYC/PVA specimens, although the diffraction patterns of α form PVA crystals can barely be found as their weight ratios of PVA to NYC of NYC/PVA specimens are less than 1/5 (i.e., $NYC_5PVA_1$and NYC_7PVA_1 samples). In contrast, it is worth noting that α form PA crystals with peak diffraction angles at 20.3° and 23.7° start to grow at the expense of the γ form PA crystals, as the weight ratios of PVA to NYC of NYC/PVA specimens are more than 1 (i.e., NYC_1PVA_1, NYC_1PVA_2 and NYC_1PVA_3 specimens).

On the other hand, the peak X-ray diffraction angle at 4.81° of NYC specimen displays the X-ray diffraction from the (001) crystal surface of the clay layers present in the NYC resin [28], which corresponds to 1.84 nm d-spacing of the clay layers. In fact, the peak diffraction angles of the clay layers reduce significantly from 4.81° to 4.09° as the weight ratios of PVA to NYC increase, which lead to an increasing d-spacing of the clay layers of the NYC/PVA specimens (see Fig. 3). Apparently, the aggregated clay layers present in NYC specimen can be dispersed by mixing PVA in NYC specimen, and hence, causes an increasing d-spacing of the clay layers as the weight ratios of PVA to NYC of the NYC/PVA specimens increase.

Thermal properties

Typical DSC thermograms of NYC, PVA and NYC/PVA specimens are shown in Fig. 4. A main melting endotherm with a peak temperature at 230.9 °C was found on the DSC thermogram of PVA resin. In contrast, the DSC thermogram of NYC specimen shows a double melting endotherm with a main melting peak temperatures at around 214 °C. Another minor melting endotherm with a higher peak temperature at around 220 °C can be found on the right shoulder of the double melting endotherm of the NYC specimen. After blending PVA in NYC, the characteristics of most DSC thermograms of NYC/PVA specimens are similar to the combination of those of the NYC and PVA specimens. However, the sizes and peak temperatures associated with the main melting endotherms of NYC and PVA reduce significantly with increasing the PVA and

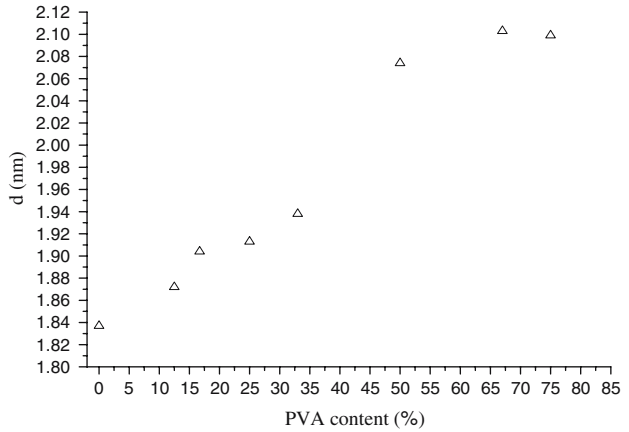

Fig. 3 The evaluated d-spacing of clay layers present in NYC/PVA specimens

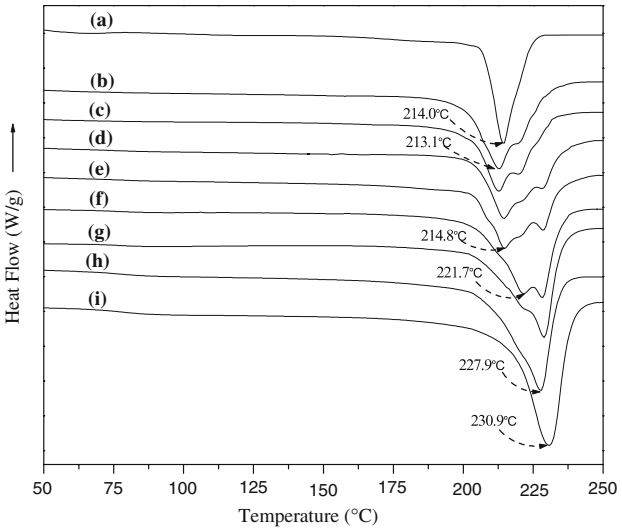

Fig. 4 DSC thermograms of (**a**) NYC, (**b**) NYC_7PVA_1, (**c**) NYC_5PVA_1, (**d**) NYC_3PVA_1, (**e**) NYC_2PVA_1, (**f**) NYC_1PVA_1, (**g**) NYC_1PVA_2, (**h**) NYC_1PVA_3 and (**i**) PVA specimens

NYC contents of NYC/PVA specimens, respectively. On the other hand, it is interesting to note that the sizes of the minor but higher melting endotherm of the NYC resin grow at the expense of the main but lower melting endotherm as the PVA contents of NYC/PVA specimens increase. In fact, the lower melting endotherm originally shown on the double melting endotherm of the NYC resin can barely be seen as the weight ratios of PVA to NYC of NYC/PVA specimens are equal to or more than 1 (i.e., NYC_1PVA_1, NYC_1PVA_2 and NYC_1PVA_3 samples). Similarly, the melting endotherm of PVA present in NYC/PVA specimens disappears quickly as their NYC contents increase. Almost no PVA melting endotherm can be found on the DSC thermograms of NYC/PVA specimens, as the PVA contents of NYC/PVA specimens are less than 16.7 wt% (i.e., $NYC_5PVA_1$and NYC_7PVA_1 samples).

Fourier transform infrared spectra

Typical Fourier transform infrared spectra (FTIR) of NYC and PVA samples are summarized in Fig. 5. Similar to those found in the literatures [22, 29–33], the distinguished absorption bands of NYC specimens centered at 1549, 1640, 2857, 2928, 3090 and 3295 cm^{-1} are most likely corresponding to the motions of N-H bending vibration, hydrogen-bonded C=O stretching vibration, symmetric CH_2 stretching vibration, asymmetric CH_2 stretching vibration, aromatic C–H stretching vibration, hydrogen-bonded N–H stretching vibration present in NYC molecules, respectively. As reported by Holland and coauthors [34, 35], the FT–IR spectra of PVA exhibit distinguished absorption bands centered at 2939 and 3328 cm^{-1}, which are attributed to the motions of C–H stretching vibration and hydrogen-bonded O–H stretching vibration, respectively. After blending PVA in NYC, the peak wave numbers of the absorption bands corresponding to the hydrogen-bonded N–H stretching of NYC molecules shift from 3295 to 3301 cm^{-1} as the PVA contents of NYC/PVA specimens increase from 0 to 75 wt%. Similarly, the peak wave numbers of the hydrogen-bonded O–H stretching bands increase significantly from 3328 to 3423 cm^{-1} as the NYC contents of NYC/PVA specimens increase from 0 to 75 wt%. In fact, as shown in Fig. 5(b, c), the hydrogen-bonded O–H stretching bands originally present in PVA specimen disappear completely as the NYC contents of NYC/PVA specimens are more than 83.3 wt% (i.e., NYC_7PVA_1 and NYC_5PVA_1 specimens).

Figures 6–9 exhibit the FT–IR spectra of NYC, PVA and NYC/PVA specimens determined at varying temperatures. It is interesting to note that the absorption bands corresponding to the hydrogen-bonded N–H (3650–3000 cm^{-1}) and C=O stretching (1800–1450 cm^{-1}) of NYC specimen and O–H stretching (3700–3300 cm^{-1}) of PVA specimen shift to higher frequencies as the testing temperatures increase, wherein the intensities associated with the hydrogen-bonded absorption bands reduce slightly with increasing the temperature. For instance, the peak wave numbers of the N-H, C=O and O–H stretching absorption bands increase from 3298 to 3312 cm^{-1}, 1638 to 1642 cm^{-1} and 3329 to 3402 cm^{-1} as the testing temperatures increase from 30 to 230 °C, respectively. Moreover, newly developed slightly absorption bands of free (nonhydrogen-bonded) amide and carbonyl groups centered at 3444 and 1668 cm^{-1} of NYC specimens and hydroxyl groups centered at 3618 cm^{-1} of PVA specimen become more pronounced as the testing temperatures increase. As shown in Fig. 10, the frequency difference (Δv) between the absorption bands of hydrogen-bonded and free amide,

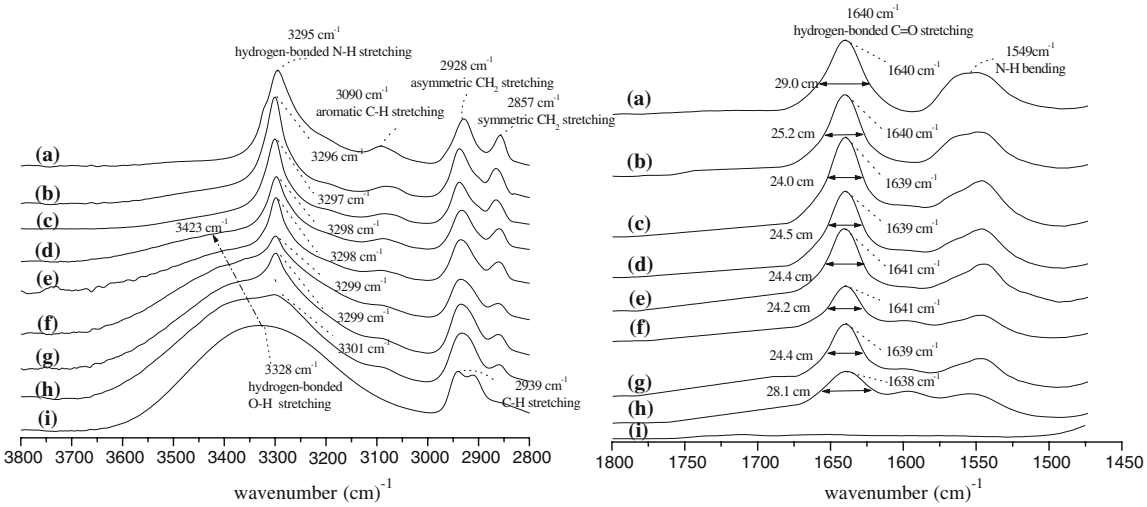

Fig. 5 FT–IR spectra of (**a**) NYC, (**b**) NYC_7PVA_1, (**c**) NYC_5PVA_1, (**d**) NYC_3PVA_1, (**e**) NYC_2PVA_1, (**f**) NYC_1PVA_1, (**g**) NYC_1PVA_2, (**h**) NYC_1PVA_3 and (**i**) PVA specimens determined at 20 °C

carbonyl and/or hydroxyl groups reduce significantly with increasing temperatures. Presumably, the shifting of the hydrogen-bonded N-H, C=O and O–H stretching bands into higher frequencies and the decrease in Δv is attributed to the gradually weakened hydrogen bonds between the amide/carbonyl groups and hydroxyl groups present in the PA6 and PVA molecules, respectively, and hence, causes the absorption band of free amide, carbonyl and hydroxyl groups become more pronounced.

On the other hand, as shown in Fig. 5, the widths shown in the half-height of the C=O stretching bands of NYC/PVA specimens reduce significantly with increasing the PVA contents. It is generally recognized that this reduction in Δw of the C=O stretching band can be attributed to the decreasing amounts of allowed C=O stretching vibrations [36]. Presumably, the decreasing allowed C=O stretching vibrations can be attributed to the gradually strengthened interaction between the carbonyl and hydroxyl groups in the NYC/PVA specimen as the weight ratios of PVA to NYC increase. Based on these premises, it is reasonable to suggest that the presence of PVA in NYC can interfere, break the hydrogen-bonded carbonyl groups originally present in NYC resins, and even form new interactions between the carbonyl and hydroxyl groups as the weight ratios of NYC to PVA of NYC/PVA specimens increase. The strengthened interaction between the carbonyl and hydroxyl groups appears to reach the maximum level as the PVA contents reach about 16.7 wt%. As a consequence,

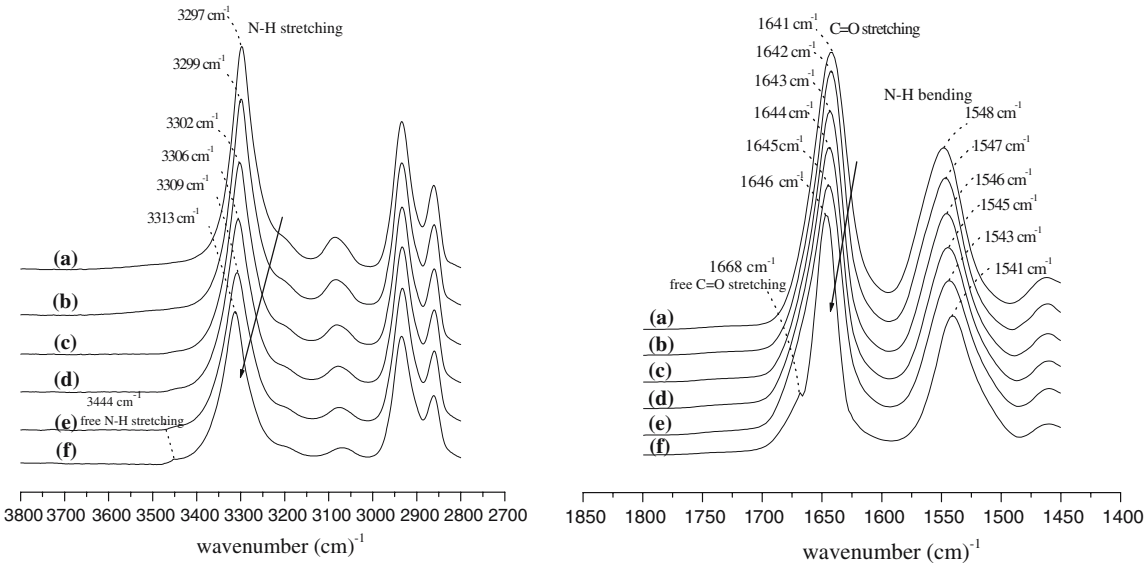

Fig. 6 FT–IR spectra of NYC specimens determined at (**a**) 30 °C, (**b**) 80 °C, (**c**) 130 °C, (**d**) 180 °C, (**e**) 210 °C and (**f**) 230 °C

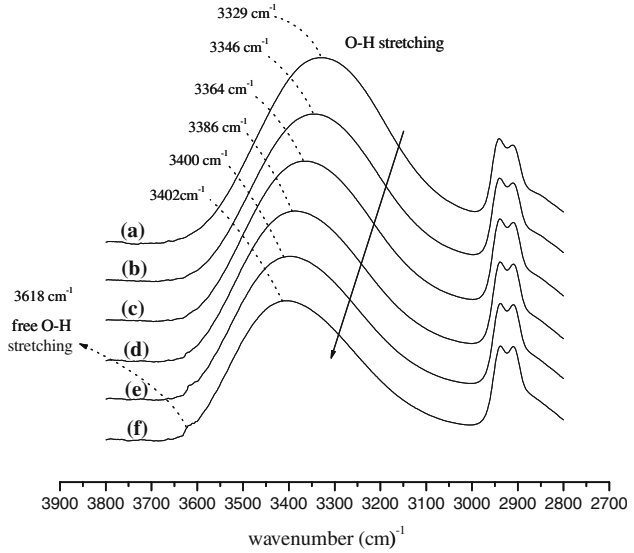

Fig. 7 FT–IR spectra of PVA specimens determined at (**a**) 30 °C, (**b**) 80 °C, (**c**) 130 °C, (**d**) 180 °C, (**e**) 210 °C and (**f**) 230 °C

the Δw values of the C=O stretching band reach the minimum and the hydrogen-bonded hydroxyl band originally present in PVA resins completely, when the PVA contents reach about 16.7 wt%.

These interesting thermal, X-ray diffraction and FTIR properties suggest that PVA molecules are miscible with PA molecules present in the NYC resin to some extents, since the characteristics of melting endotherm, X-ray diffraction patterns of α form PVA crystals and hydrogen-bonded hydroxyl groups originally associated with the PVA resin almost disappear after blending less than 16.7 wt% of PVA in NYC resins. However, at PVA contents more than 16.7 wt%, the ''over saturated'' PVA molecules appear to be present as the separate phases in NYC/PVA specimens. It is, therefore, the characteristics of melting endotherm, X-ray diffraction of α form PVA crystals and hydrogen-bonded hydroxyl groups originally associated with the PVA resins appear gradually as the PVA contents of NYC/PVA specimens are more than 16.7 wt%.

Presumably, the degrees of molecular interaction originally present in PVA molecules can be significantly higher than those present in PA molecules, since the amounts of strongly hydrogen-bonded hydroxyl groups present in PVA resins are expected to be much more than those of hydrogen-bonded carbonyl and amide groups present in NYC resins. Similarly, the degrees of molecular interaction present in NYC/PVA blends are expected to increase as their PVA contents increase, because the ''over saturated'' PVA molecules appear to be present as the separate phases in NYC/PVA specimens as their PVA contents are more than 16.7 wt%. The gradually strengthened molecular interaction of separated PVA phases can significantly increase the time and difficulty of melt-processing the NYC/PVA blends before they reach the stabilized status, and hence cause significantly increase in values of the torque and ''stabilized'' time as their PVA contents are more than 16.7 wt%. In fact, as evidenced in Fig. 1, the additional demarcated humps and significantly increased torques and ''stabilized'' time values clearly indicate the difficulty of melt-processing the NYC/PVA blends as their PVA contents are more than 50 wt%. However, as described previously, the characteristics of melting endotherm, X-ray diffraction patterns of α form PVA crystals and hydrogen-bonded hydroxyl groups originally associated with the PVA resin can barely be seen after blending less than 16.7 wt% of PVA in NYC resins. Under such

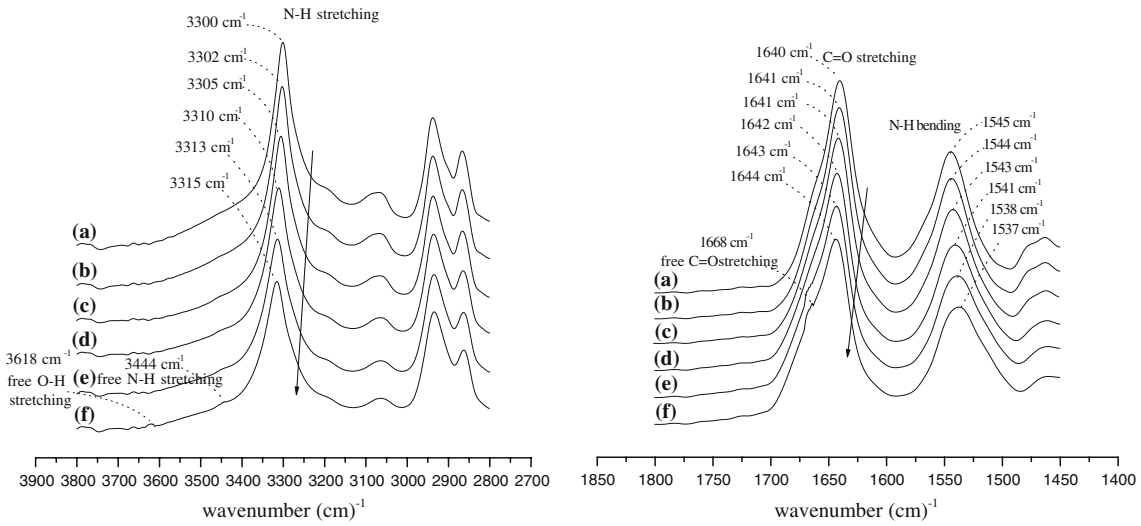

Fig. 8 FT–IR spectra of NYC_5PVA_1 specimens determined at (**a**) 30 °C, (**b**) 80 °C, (**c**) 130 °C, (**d**) 180 °C, (**e**) 210 °C and (**f**) 230 °C

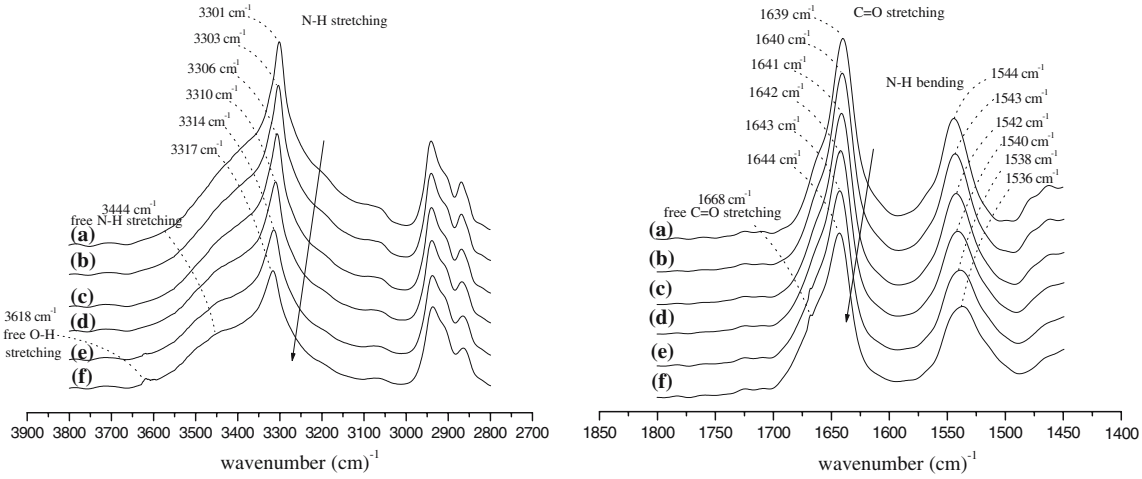

Fig. 9 FT–IR spectra of NYC_1PVA_1 specimens determined at (**a**) 30 °C, (**b**) 80 °C, (**c**) 130 °C, (**d**) 180 °C, (**e**) 210 °C and (**f**) 230 °C

circumstances, it is reasonable to believe that PVA molecules are miscible with PA molecules in the molecular level as the PVA contents are less than 16.7 wt%. As a consequence, only slight increase in the values of ''stabilized'' time and torque of NYC/PVA blends was found as their PVA contents increase from 0 to 16.7 wt%, since the ''tractable'' hydrogen-bonded hydroxyl groups originally present in PVA molecules are barely exist in NYC/PVA blends.

On the other hand, as suggested by several investigators [23–25], protonated amino end groups of PA molecules can be ionically bonded to the surfaces of negatively charged silicate sheets, which then leads to a poorly arranged PA conformation gathered on the surfaces of the silicate sheets. These poorly arranged PA molecules are then served as the nucleation sites, and hence, cause the formation of γ form

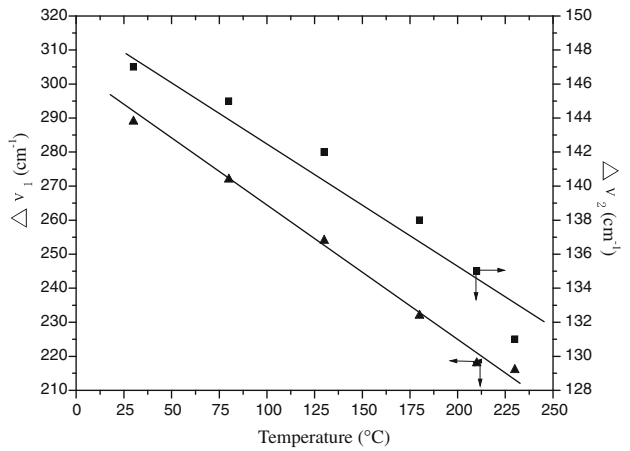

Fig. 10 Frequency difference (Δv_1) between the absorption bands of hydrogen-bonded hydroxyl and free hydroxyl groups of PVA specimens (▲) and Frequency difference (Δv_2) between the absorption bands of hydrogen-bonded amide and free amide groups of NYC specimens (■) determined at varying temperatures

PA crystals during the crystallization processes of NYC melts, although the α form PA crystals with PA molecules linearly aligned in the unit cells are the more stable form. It is also suggested [37] that the lower and higher melting endotherm found on the DSC thermograms of NYC and NYC/PVA specimens are due to the melting of the γ form and the recrystallized α form PA crystals, respectively, since more energies can be supplied at higher temperatures to overcome the restriction and transform parts of the γ form PA crystals to α form during the DSC heat scanning processes. However, PVA molecules are expected to have much more protonated hydroxyl end groups to interact with the negatively charged silicate sheets than PA molecules. At relatively high PVA contents, the protonated hydroxyl end groups of the PVA molecules can replace the amino end groups and be ionically bonded to the surfaces of negatively charged silicate sheets, which then free the poorly arranged PA conformation originally gathered on the surfaces of the silicate sheets, and hence, cause the formation of the more stable α form PA crystals during the crystallization processes of NYC/PVA melts as the PVA contents are equal to or more than 50 wt%. It is, therefore, α form PA crystals continue to grow at the expense of γ form PA crystals as the PVA contents of NYC/PVA specimens increase, and the characteristics of the γ form PA crystals originally shown on the melting endotherm and X-ray diffraction patterns of the NYC resin can barely be seen as the PVA contents of NYC/PVA specimens are equal to or more than 50 wt%.

Mechanical properties

The tensile properties of NYC, PVA and NYC/PVA specimens are summarized in Fig. 11. The NYC specimen exhibit significantly lower tensile strength (σ_f) (43 vs.

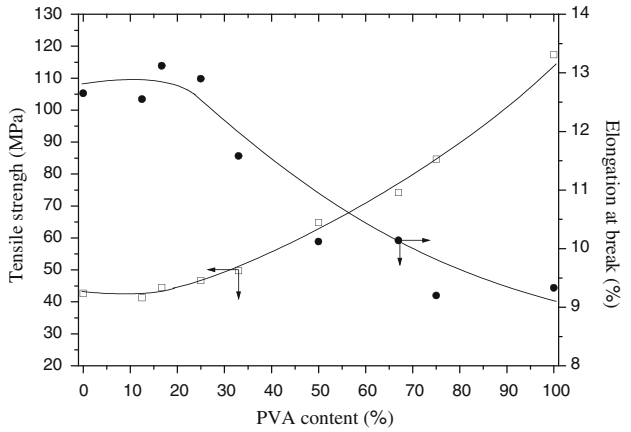

Fig. 11 The values of tensile strength (□) and elongation at break (●) of NYC, PVA specimens and NYC/PVA specimens

116 MPa) but slightly higher elongation at break (ε_f) (12.5 vs. 9.4%) than PVA specimen. Somewhat interestingly, after blending PVA in NYC, the σ_f and ε_f values of NYC/PVA specimens remain relatively unchanged initially with increasing the PVA contents. For instance, the σ_f and ε_f values of NYC/PVA specimens increase only slightly from 43 MPa/12.5% to 44 MPa/13.1% as their PVA contents increase from 0 to 16.7 wt%. However, their σ_f and ε_f values increase and reduce significantly from 44 MPa/13.1% to 116 MPa/9.4% as the PVA contents of NYC/PVA specimens increase from 16.7 to 100 wt%, respectively. These results clearly support the ideas that PVA molecules are miscible with PA molecules to some extents in the molecular level as the PVA contents of NYC/PVA specimens are less than 16.7 wt%. Based on these premises, it is reasonable to believe that the tensile properties of NYC/PVA specimens are nearly the same as those of the NYC specimen. However, the gradually grown separated PVA phase make the tensile properties of NYC/PVA specimens to behave more like those of the PVA specimen as their PVA contents reach more than 16.7 wt%.

Conclusion

The thermal, X-ray diffraction and FTIR properties of NYC/PVA specimens suggest that PVA molecules are miscible with PA molecules in NYC resins to some extents, since the characteristics of melting endotherm, X-ray diffraction patterns of α form PVA crystals and hydrogen-bonded hydroxyl groups originally associated with the PVA resin almost disappear after blending less than 16.7 wt% of PVA in NYC resins. It is suggested that the presence of PVA in NYC can interfere, break the hydrogen-bonded carbonyl groups originally present in NYC resins, and even form new interactions between the carbonyl and hydroxyl groups as the weight ratios of NYC to PVA of NYC/PVA specimens increase. As evidenced by FTIR analysis, the strengthened interaction between the carbonyl and hydroxyl groups appears to reach the maximum level as the PVA contents are equal to 16.7 wt%. However, the characteristics of melting endotherm, X-ray diffraction of α form PVA crystals and hydrogen-bonded hydroxyl groups originally associated with the PVA resins appear gradually as the PVA contents of NYC/PVA specimens are more than 16.7 wt%. These results clearly suggest that the ''over saturated'' PVA molecules gradually appear as the separate phases in NYC/PVA specimens as their PVA contents are more than 16.7 wt%. The torques vs. time measurements and tensile properties of NYC/PVA specimens both support the ideas that PVA molecules are miscible with PA molecules to some extents in the molecular level as the PVA contents of NYC/PVA specimens are less than 16.7 wt%. Moreover, the additional demarcated humps and significantly increased torques and ''stabilized'' time values support the presence of separated PVA phases in NYC/PVA specimens as their PVA contents are more than 50 wt%. On the other hand, It is worth noting that the α form PA crystals continue to grow at the expense of γ form PA crystals as the PVA contents of NYC/PVA specimens increase, and the characteristics of the γ form PA crystals originally shown on the melting endotherm and X-ray diffraction patterns of the NYC resin can barely be seen as the PVA contents of NYC/PVA specimens are equal to or more than 50 wt%. Presumably, at relatively high PVA contents, the relatively high degrees of protonated hydroxyl end groups of the PVA molecules can replace and free the poorly arranged PA conformation originally gathered on the surfaces of the silicate sheets, and hence, cause the formation of the more stable α form PA crystals during the crystallization processes of NYC/PVA melts as the PVA contents are equal to or more than 50 wt%.

References

1. Olabisi O, Robeson LM, Shaw MT (1979) Polymer-polymer miscibility. Academic Press, New York
2. Paul DR, Newman S (1978) Polymer blends. Academic Press, New York
3. Lee CF (2000) Polymer 41:1337
4. Kohan MI (ed) (1973) Nylon plastics. Wiley-Interscience, New York
5. Finch CA (1992) Polyvinyl alcohol, chapters 1–3 and 12–18. Wiley, New York
6. Nakano N, Yamane S, Toyosima K (1989) Poval(polyvinyl-alcohol), chapter 3. Japan Polymer Society, Kyo To
7. Jang J, Lee DK (2003) Polymer 44:8139
8. Casey JP, Manley GB (1978) Proceedings of 3rd international biodegradable symposium. Applied Science Publishers, London
9. Ikejima T, Cao A, Yoshie N, Inoue Y (1998) Polym Degrad Stab 62:463

10. Gajria AM, Dave V, Gross RA, McCarthy SP (1996) Polymer 37:437
11. Koulouri EG, Kallitsis JK (1998) Polymer 39:2373
12. Usuki A, Koiwai A, Kojima Y, Kawasumi M, Okada A, Kurauch T, Kamigaito O (1995) J Appl Polym Sci 55:119
13. Okada A, Fukushima Y, Kawasumi M, Inagaki S, Usuki A, Sugiyama S, Kurauc Th, Kamigaito O (1988) US Patent 4, 739, 007
14. Kojima Y, Usuki A, Kawasumi M, Okada A, Fukushima Y, Kurauchi T, Kamigaito O (1992) J Mater Res 8:1185
15. Morgan AB, Gilman JW, Harris RH, Jackson CL, Wilkie CH, Zhu J (2000) Polym Mater Sci Eng 83:53
16. Kojima Y, Usuki A, Kawasumi M, Okada A, Kurauchi T, Kamigaito O (1993) Appl J Polym Sci 49:1259
17. Michaels AS, Chandrasekaran SK, Shaw JE (1975) AICHE J 21:985
18. Wakeman WA, Mason EA (1979) Ind Eng Chem 18:301
19. Cussler EL, Hughes SE, Ward WJ, Aris R (1988) J Membrane Sci 38:161
20. Falla WR, Mulski M, Cussler EL (1996) J Membrane Sci 119:129
21. Yang CF, Nuxoll EE, Cussler EL (2001) AICHE J 47:295
22. Yeh JT, Yao WH, Chen CC (2005) J Polym Res 12:279
23. Liu L, Qi Z, Zhu X (1999) J Appl Polym Sci 71:1133
24. Liu X, Wu Q (2002) Polymer 43:1933
25. Pinnavaia TJ, Beall GW (2000) Polymer-clay nanocomposites. John Wiley and Sons, New York
26. Wu TM, Chen EC (2002) Polym Eng Sci 42:1141
27. Konishi Y, Cakmak M (2005) Polymer 46:4811
28. Jiang T, Wang YH, Yeh JT, Fan ZQ (2005) Eur Polym J 41:459
29. Akrovanek DJ. Howes SE, Painter PC, Coleman MM (1985) Macromolecules 18:1676
30. Deimede VA, Fragou KV, Koulouri EG, Kallitsis JK, Voyiatzis GA (2000) Polymer 41:9095
31. Arimoto H (1964) J Polym Sci: Part A 2:2283
32. Schroeer LR, Cooper SL (1976) J Appl Phys 47:4310
33. Yeh JT, Yao WH, Du QG, Chen CC (2005) J Polym Sci: Part B 43:511
34. Holland BJ, Hay JN (2002) Polymer 43:2207
35. Holland BJ, Hay JN (2001) Polymer 42:6775
36. Person WB, Zerbi GE (1982) Vibrational intensities in infrared and Ramam Spectroscopy. Elsevier, New York
37. Lincoln DM, Vaia RA, Wang ZG, Hsiao BS (2001) Polymer 42:1621